Preferential flow behaviour in unsaturated packed beds and heaps: Incorporating into a CFD model

D. McBride, I.M.S.K. Ilankoon, S.J. Neethling, J.E. Gebhardt, M. Cross

PII: S0304-386X(16)30546-1
DOI: doi: 10.1016/j.hydromet.2017.06.008
Reference: HYDROM 4600

To appear in: *Hydrometallurgy*

Received date: 12 August 2016
Revised date: 26 April 2017
Accepted date: 3 June 2017

Please cite this article as: D. McBride, I.M.S.K. Ilankoon, S.J. Neethling, J.E. Gebhardt, M. Cross , Preferential flow behaviour in unsaturated packed beds and heaps: Incorporating into a CFD model, *Hydrometallurgy* (2017), doi: 10.1016/j.hydromet.2017.06.008

Preferential flow behaviour in unsaturated packed beds and heaps: Incorporating into a CFD model

*D. McBride[1], I.M.S.K. Ilankoon[2], S.J. Neethling[3], J.E.Gebhardt[4], M.Cross[1]

[1] College of Engineering
Swansea University, Bay Campus, Swansea SA1 8EN, Wales UK
(*Corresponding author: d.mcbride@swansea.ac.uk)

[2] Discipline of Chemical Engineering, School of Engineering
Monash University, Jalan Lagoon Selatan
47500 Bandar Sunway, Selangor Darul Ehsan, Malaysia

[3] Department of Earth Science and Engineering,
Royal School of Mines, Imperial College London, London SW7 2AZ, UK

[4] FLSmidth Inc., Salt Lake City, Utah USA

ABSTRACT

Heap leach stockpiles inevitably contain local voidage heterogeneities due to non-uniform particle size distributions of the ore and other factors that lead to preferential flow paths and solution channelling. The stockpile can also encounter diverse flow conditions due to a number of factors, including storm events, infiltration into dry ore material, cyclic drain down, compaction, migration of fines, all contributing to large variations in local ore permeability and the creation of preferential flow pathways. Non-uniform and adverse flow behaviour within the heap reduces the leaching efficiency which can lead to lower metal recoveries. Therefore, capturing the local flow variations that affect the transport of leach solution within the heap is critical to accurately predicting the leaching kinetics. Experimental data shows how channelling develops due to local heterogeneities that cannot be eliminated by packing alone. Thus, effective modelling of heap leach stockpiles should account for these channelling affects. This paper utilises a robust computational fluid dynamics (CFD) framework that incorporates techniques to account for local preferential flow paths in the heap leach system. The results are compared against liquid flow behaviour in a pseudo two-dimensional column of narrowly sized particles and a more realistic particle size distribution. The methods are then applied to a hypothetical leach to assess the impact of accounting for the flow variability in the heap.

KEYWORDS
Heap leaching, preferential flow, channelling, Computational fluid dynamics (CFD), Hydrodynamics

1. INTRODUCTION

Heap leaching is often the preferred method for the extraction of base and precious metals from large volumes of low grade mineral deposits. This method provides a cost effective technique for the recovery of a range of metals, such as copper, gold, zinc and uranium from low grade ores. However, the efficiency of recovery can be quite variable with recovery rates typically ranging from 50% – 80%, with the more complex sulphide deposits providing lower

yields than a typical oxide deposit. While leaching effectiveness is influenced by a range of factors, including surface chemistry, mass and heat transfer and biological activity (Petersen, 2015), poor hydrodynamic performance within the heap is often a key factor in low overall recoveries.

Stockpile leaching is a physico-chemical process, typically irrigating a crushed stockpile of low grade ore with a leaching solution. An overview of leaching technologies is given by Bartlett (1992) and a review of its current state and future direction is given by Ghorbani et al (2016). A lixiviant is applied to the top exposed surface of the stockpile and the solution percolates through the ore dissolving the metals from the rock often giving rise to complex hydrothermal chemical interactions The dissolved metal in solution is then transported out of the base of the stockpile and into collection ponds for further processing to extract the valuable metals. For optimum recovery, the stockpile should have good hydrodynamic properties as local variability in liquid transport within the heap can limit the leach reaction kinetics and result in non-wetted and/or stagnant regions. Solution flow can be influenced by porosity of the packed particles, local voidage variability, changes in packing, compaction of the ore, percentage of fines and migration of fines within the heap. As Kunkel (2008) states, the recovery of the metal from the ore is more about the solution flow characteristics than the material, and unsaturated flow characteristics in heaps are more about the material than the fluids.

Low liquid irrigation rates and the use of dripper emitters contribute to the non-uniformity and complexity of the resultant unsaturated flow conditions. Large rain events can increase the formation of channels and saturated regions within the heap. The solution spreads through the heap by formation of flow paths between particles driven by gravity and horizontal spread due to the capillary action of the micro-pores of the particles, as well as the dispersion due to the tortuous paths that the flow must follow. The Bond number, which is the ratio of gravity to capillary forces, is typically around one for gravity driven flow around the particles and many orders of magnitude less than one for capillary driven flow within the particles. These differences in length scales produce complex flow behaviours within the heap (Ilankoon and Neethling, 2012, 2013, 2016). Ideally, the uniform application of lixiviant would lead to a uniform wetting of particles. However, in practice the liquid applied to the top of the heap is not uniform and percolates through the heap along preferential channels (Petersen and Dixon, 2007). Solution is generally applied by drip emitter lines, typically spaced about 50 cm apart to cover a targeted wetted area of approximately 0.25 – 1 m^2. A reduction in the spacing may lead to increased uniformity of wetting (Afewu, 2009), though it will not completely eliminate flow variability and has to be balanced against other factors (typically cost related).

Strong structural heterogeneity and density changes across the heap due to particle segregation have been observed (Howard, 1968, Roman 1977, Yusuf, 1984, Bartlett, 1992). Localized pockets of high and low permeability regions often lead to preferential flow channels (Yusuf, 1984). Flow channelling associated with strong structural heterogeneity that may occur over time has been observed in small scale laboratory columns and large scale heaps (Howard, 1968, Armstrong et al, 1971, Murr, 1979, Cathles and Murr, 1980, Murr et al, 1981, Wu et al. 2007, 2009, Fagan et al, 2014, Ilankoon and Neethling, 2016). When solution flows through preferential channels in the stockpile, the metal recovered is reduced due to limited solution-ore contact in regions away from these channels. This can be the principle factor in reducing metal recovery in some stockpiles (Wu et al., 2007, 2009). Zhan et al. (2012) presented a summary of analytical and field studies, concluding that the

development of channelling and preferential flow paths in large heaps leads to incomplete mixing and a reduction in metal recovery.

Many researchers have employed numerical techniques in order to predict the flow and leach behaviour within a heap. Among the authors that have presented fluid flow models and investigated the hydrodynamic behaviour of the heap, are Munoz et al. (1997), Bouffard and Dixon (2001), Pantelis et al. (2002), Cariaga et al. (2005), Peterson and Dixon (2007), and Guzman et al. (2013). Dixon and Petersen (2003) presented a model for column heap leaching using a model based on raffinate diffusing out to reaction sites from discrete channels through the ore and used comparisons to column test results to generate confidence in the model for predictions of behaviour in heaps. Computational Fluid Dynamics (CFD) technologies have enabled more complex multiphase transport in the modelling of the heap leaching process (Leahy et al., 2005, 2006, 2007; Leahy and Schwarz, 2009; Wu et al., 2010; Garcia et al., 2010; Bennett et al., 2012; Gebhardt et al., 2012; McBride et al., 2014, 2016). Cariaga et al. (2005) employed a mixed hybrid finite-element approach for two-phase flow in a two-dimensional heap. Mostaghimi et al. (2014a, 2014b) employed a control volume finite element method with mesh adaptivity in three-dimensions to capture the hydrodynamics of heap leaching process at large scale. The control volume finite volume method has also been applied to full scale three-dimensional industrial oxide heaps by McBride et al. (2012a, 2012b). Many authors employ soil-water retention curves to obtain the unsaturated soil hydraulic parameters to model the hydrodynamics of the heap. This requires fitting of data and/or some calibration of the model to experimental tests (McBride et al., 2013; Cariaga et al., 2015). In the modelling of heap leach systems, homogeneous ore properties or bulk heterogeneous ore properties are normally assumed (i.e., macro uniform voidage per material). However, in the modelling of preferential and non-equilibrium flow and transport in the vadose zone a range of numerical approaches have been proposed to account for spatial heterogeneity and are reviewed by Simunek et al. (2003). Although it is acknowledged that preferential flow paths have a significant effect on the leaching kinetics of the heap, this phenomena is often ignored by heap leach modellers and scale up factors are employed from small scale predictions to large scale heaps. An attempt to include the effect of preferential flow paths was included in the modelling work of McBride et al. (2012a, 2012b), who employed bulk heterogeneous materials.

This paper employs a hydrodynamics model coupling variably saturated zone hydrology with CFD technology (McBride et al., 2006). The numerical procedure is based on the mixed form of the classical Richards' equation, employing an adaptive transformed mixed algorithm that is numerically robust and significantly reduces compute (or CPU) time. This paper investigates incorporating techniques into the model to account for preferential flow paths in the heap leach system via randomly applied voidage and source-sink terms. The approach of adding source and sink terms to the CFD model to incorporate local transport between different flow regions have been employed by Bujalski et al (2000, 2005). In their formulation source terms represented transport between flowing and stagnant regions. In this paper the source term represents transport from the ore matrix into gravity driven open channels. The focus of this paper is to capture the wetting behaviour and liquid flow path development (i.e., channelling) that occurs in heap leaching processes. The numerical predictions are compared with published experimental results (Ilankoon and Neethling, 2016). The experiments are designed to investigate the liquid spread mechanisms in packed beds and heaps using a laboratory scale pseudo 2-D system of both narrowly sized and realistic particle size distributions. The numerical technique is shown to implicitly account for the effects of flow channelling by reducing the solution-ore wetting by channelling flow

outside the matrix when uniform permeability/voidage has been assumed. However, to fully capture the flow channelling features, a dual permeability formulation incorporating local permeability/voidage variations is investigated. The effect on leaching kinetics is then illustrated by simulating a hypothetical solute transport with a simple reaction.

2. COMPUTATIONAL MODEL

The heap leach model has been implemented within an in-house multi-physics computational fluid dynamics (CFD) framework. The multi-physics environment PHYSICA provides a three-dimensional finite volume unstructured mesh modular framework (Croft et al., 1995). The governing equations are discretised over a solution domain, a three dimensional mesh comprised of a mix of tetrahedral, wedge and hexahedral elements, employing cell-centred finite volume approximations. The computational procedure employed for the solution of unsaturated-saturated flow through the porous media is based on the mixed form of the classical Richards' equation. The method is numerically robust, employing an adaptive transformed mixed algorithm on a three-dimensional finite volume unstructured mesh framework. A detailed description of the algorithm is given in McBride et al. (2006). The liquid flow is coupled with transport equations within the CFD framework.

2.1 Flow in porous media

The variably saturated liquid flow through the porous media is modelled by solving the mixed form of the Richards' equation (1) (Richards, 1931, McBride et al. 2006). In this formulation, the influence of air on the movement of liquid is assumed to be insignificant, thus the gas flow does not influence the liquid flow but the fluid flow can influence the movement of gas. The mixed form contains terms for the moisture content, θ (m^3/m^3) defined as the volume of liquid / total volume of solid-liquid-air space, and water pressure head, *h*.

$$\frac{\partial \theta}{\partial t} = \nabla\left[K(h)\nabla h\right] + \frac{\partial K(h)}{\partial z} + S \tag{1}$$

In equation (1), *K(h)* is the hydraulic conductivity, which is a function of the pressure head (or capillary-suction), *z* is the direction of gravity, *t* is time and *S* is a source term which also includes the boundary conditions.

The effect of solution channelling, where lixiviant travels through the media with limited solution-ore wetting, is incorporated into equation (1) as an additional volume sink/source, which is calculated as an area flux through the inlet area of a preferential flow channel. The source term is re-written as;

$$S = S_{BC} + S^{cl} \tag{2}$$

where S_{BC} contains the boundary condition and volume source terms and S^{cl} acts as a sink term that represents the transfer rate of the liquid from the matrix into preferential flow channels. The channelled liquid passes along preferential paths without interacting with the ore matrix. The channelled solution sink term depends upon the local hydraulic properties of the media and saturation levels within the ore;

$$S^{cl} = \nabla\,(k(h)\nabla H) \tag{3}$$

where H is the total hydraulic head and z is the gravitational head, with $H=h+z$, thus eqn (3) can be written as;

$$S^{cl} = \nabla\,(k(h)\nabla h) + \nabla\,(k(h)\nabla z) \tag{4}$$

In the simulations reported here, the inlet face area, A_{cf}, of the channel is assumed to be equal to the face area of the element containing the sink term with normal in the direction of gravity. The pressure head gradient on a preferential flow channel face is assumed to vary predominately in the direction of gravity, thus only the z direction is significant. Therefore integrating eqn (4) over elements containing the preferential flow channels and applying Gaussian theory, the discretised S^{cl} becomes;

$$S^{cl} = \sum_{cf}\left(K(h)\frac{\partial h}{\partial z} + K(h)\frac{\partial z}{\partial z}\right)A_{cf}.n_z = \sum_{cf}\left(K(h)\frac{\partial h}{\partial z} + K(h)\right)A_{cf}.n_z \tag{5}$$

where n_z is the face normal in the direction of gravity.

In the formulation here the local pressure head is assumed constant and the channelled liquid is returned to the medium at the outlet element in the direction of gravity. However, the channelled solution could enter and leave the medium via the pressure head gradient but this would require solution of the pressure head in the channels. The S^{cl} source term can be applied locally to elements on a specified or random basis.

The volume of solution entering a channelled pathway is tracked and the time, t, taken for it to move through an elevation, z, will depend upon the tortuosity, τ, of the preferential paths. The solute is assumed to travel at a speed proportional to the saturated hydraulic conductivity of the local media, $t = z\,\tau/K_{sat,}$ where K_{sat} is the saturated hydraulic conductivity.

The solution of equation (1) requires relationships for pressure head – liquid content – hydraulic conductivity to be specified to describe the moisture characteristics of the porous media. The unsaturated moisture content $\theta(h)$ and hydraulic conductivity $K(h)$ are nonlinear functions of the pressure head and are represented here, equations (6) and (7) by the van Genuchten-Mualem model (van Genuchten, 1980);

$$\theta(h) = \begin{cases} \theta_{res} + \frac{\theta_{sat}-\theta_{res}}{[1+|\alpha h|^n]^m}, h < 0 \\ \theta_{sat},\ h \geq 0 \end{cases} \tag{6}$$

$$K(h) = K_{sat}\left[\frac{\theta(h)-\theta_{res}}{\theta_{sat}-\theta_{res}}\right]^L\left[1-\left(1-\left[\frac{\theta(h)-\theta_{res}}{\theta_{sat}-\theta_{res}}\right]^{1/m}\right)^m\right]^2 \tag{7}$$

where θ_{sat} is the saturated moisture content, θ_{res} is the residual moisture content, L is a pore tortuosity/connectivity dimensionless parameter normally assumed to be 0.5 (Mualem, 1976) but is often negative when empirically fitted. Schaap and Leij (2000) found that to insure a physically realistic relationship the constraint $L > -2 - 2/(n-1)$ should be employed, α is related to the inverse of the air-entry pressure, n is a measure of the pore-size distribution and $m = 1 - 1/n$.

The equation for the solute transport in the porous media is,

$$\frac{\partial(\theta C_i)}{\partial t} - \nabla(\theta D_{i,jk}.\nabla C_i) + \nabla(qC_i) = S_i + S_i^{cl} \quad (8)$$

where C_i is the concentration of species i in the solution phase, q is the darcy flux ($q = -K(h)\nabla H$, where H is the total hydraulic head, $H = h + z$), $_{jk}$ are (*x*,*y*,*z*) directions, S_i the production or consumption of species i, and S_i^{cl} is the moles of species entering or leaving preferential paths, $S_i^{cl} = S^{cl}\theta C_i$. The dispersion coefficient, $D_{i,jk,}$ is dependent upon the velocity components and longitudinal and transverse dispersivities. The dispersion coefficient is often estimated from experimental data or derived from a relationship between water content and water velocity, Nutzmann et al (2002) discusses some formulations. For the solute transport work given in this paper the dispersion coefficient is neglected as the experimental material did not contain fines, thus, greatly reducing the dispersion effect. However, the dispersion effect would need to be included for more realistic predictions of ores containing fines.

Water retention curves were derived from one dimensional packed bed experiments (i.e., cylindrical column flow tests). In the simulations no-flow boundary conditions were applied to the side of the column and a Newmann boundary condition to the top surface. At the outlet, a free drainage condition was imposed assuming unit pressure gradient, $(K(h)_f + k(h)_{fz})A_f n_f$, where $_f$ denotes the boundary face, z the gravity component, A the face area and n the outward normal to the boundary.

It is assumed that during the time the solute and species are travelling through a preferential pathway they have no interaction with the leaching kinetics of the ore.

3. EXPERIMENTAL SETUP AND METHODS

3.1. Flow Model Calibration Experiments

The flow model calibration experiments were carried out by Ilankoon and Neethling (2012, 2013) in a cylindrical column of diameter 243 mm and height of 500 mm. The ore system used consisted of copper ore particles collected from Kennecott Utah Bingham Canyon Mine. The fluid flow experiments were performed with both a narrowly sized fraction of ore particles (20-26.5 mm) and a more realistic ore size distribution (2-26.5 mm). Heap stockpiles contain fines i.e. a percentage of particles less than 2 mm, which are not accounted for in this investigation. These fines act as a mechanism for spreading the solution by capillary action laterally; a small percentage of fines can prevent preferential flow channels developing, however a high percentage of fines can lead to compaction and the creation of preferential flow paths. The liquid (water as this was a flow study rather than a leaching study) was evenly applied to the top of the packed bed until a steady state was reached. The packed bed was initially micro-pore saturated so fluid could only flow between the particles. Once a steady state was obtained the liquid content was measured and the column was then allowed to drain down and the residual liquid content was obtained (40 min to obtain the short-term external residual holdup, not the final long-term residual holdup). The solution was applied at an increasing rate of 1.26, 2.52, 5.04, 10.08 and 21.16 L/h, after each rate increase the bed was allowed to drain for 40 minutes. The liquid application process was then reversed and the flow rate was decreased through the same sequence of flow rates. The

lower flow rates typically corresponds to application rates found in heap leaching but within the heap local flow fluctuations will occur with higher and lower flows occurring. The higher flow rates employed in this investigation reflect the high flow rates seen directly under the drip emitter before the solution spreads and allows the effect of solution spread to be investigated on a material containing no fines. This experimental methodology is described in more detail in Ilankoon (2012) and Ilankoon and Neethling (2012, 2013).

3.2. 2-D Liquid Flow Experiments

A rectangular Perspex column with a width of 800 mm, a height of 600 mm and a depth of only 100 mm was designed (see Figure 1) by Ilankoon and Neethling (2016) in order to investigate vertical and horizontal liquid flow behaviour in ore systems and is referred to as the pseudo 2-D column due to its large horizontal aspect ratio. The fluid flow experiments were performed with a narrowly sized ore fraction (20-26.5 mm) and a more realistic ore mixture (2-26.5 mm). Typically, about 75 kg of particles were employed to randomly fill the 2-D column. Especially during the packing of the realistic mixture, the column was packed using a series of thoroughly mixed small batches, rather than pouring in the whole mixture at once, in order to minimise particle segregation within the packed bed. A single horizontal drip point was located at the centre of the top of the bed (see Figure 1). This was done to mimic the behaviour around a single dripper (the width of the 2-D column is similar to the typical spacing between drippers in an industrial heap). Liquid (water) was continuously added at 4.2 L/h for 2 weeks.

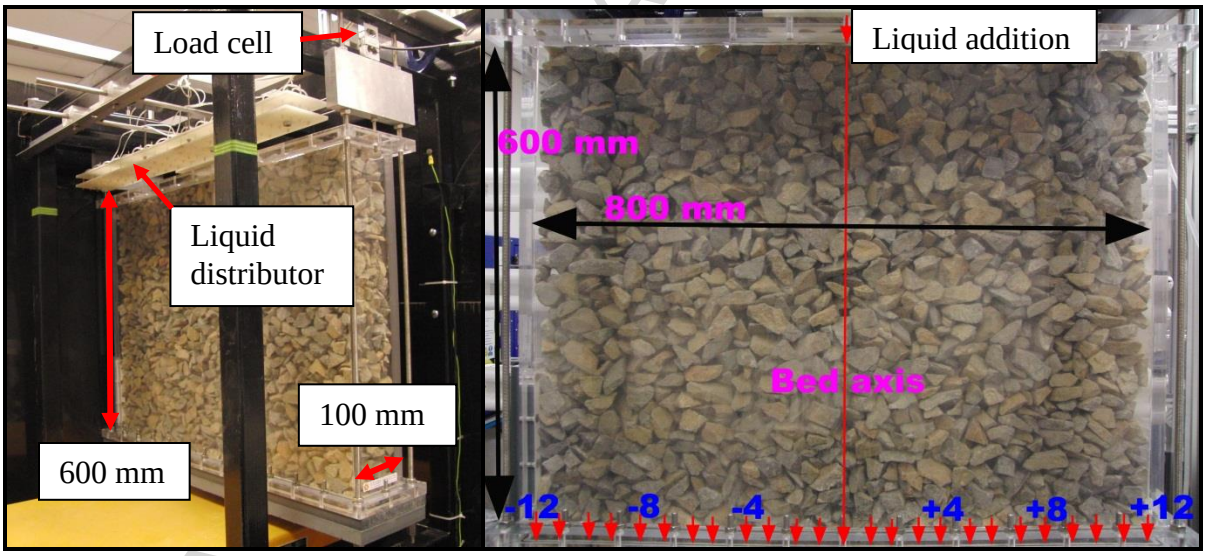

Figure 1: 2-D column rig and its main components (After Ilankoon and Neethling, 2016).

At the bottom of the column there was a series of channels (25 in total) and collection ports spaced 30 mm apart from which the out-flowing liquid was collected (see Figure 1). In all experiments, the flow from each collection port was recorded separately and the wetting of the bed was also filmed. This experimental setup and the methodology is described in more detail in Ilankoon and Neethling (2016).

4. FLOW SIMULATIONS

Material properties were obtained from experimental data, i.e. porosity, bulk voidage, permeability, Ilankoon and Neethling (2016). Model calibration simulations were performed

on a one dimensional column (i.e., cylindrical column) to fit the van Genuchten parameters, *n* and *L* to the water retention curve seen in the experiments for both the narrowly-sized and realistic-size particle distributions. The van Genuchten parameter α, which controls the spread of liquid by capillary suction, cannot be fitted in one-dimensional analysis and although there is a large volume of published work on fitting van Gunchten parameters, there has been very little work on material of large particle sizes with diameters greater than 2 mm. McBride et al (2014c) presented van Guenchten parameters for ores of various percent fines obtained from hydraulic testing. The van Guenchten parameter α ranged from 0.15 cm^{-1} to 0.3 cm^{-1} for ores with 25% fines to 15% fines. Thoma et al (2014) performed field-scale infiltration experiments on mixed coarse sand and gravel, obtaining α parameters between 0.04 cm^{-1} and 0.5 cm^{-1}. As the ore under investigation is a very coarse material with no particles less than 2mm a high value of $\alpha = 0.4\ cm^{-1}$ was employed.

Simulations were then performed on a two dimensional packed bed (Figure 1) with liquid applied to the center point of the top surface to simulate a single drip emitter. Three sets of simulations on each material were performed assuming, a) homogeneous properties on uniformly packed beds without channelling of solution, b) homogeneous material properties and packing, but with preferential flow channels i.e the channelling source term (3) was applied to local elements using a uniform probability function, and lastly c) with homogeneous material properties but with variations in packing of the ore resulting in a random voidage distribution. In the last case the average bulk voidage was kept as the previous cases but the local voidage values were randomly distributed using a uniform probability function with a maximum and minimum value of plus or minus 50% of the average bulk value. As an increase in voidage will also increase the area available for flow the hydraulic conductivity was also adjusted assuming a linear void ratio versus log permeability relationship (Taylor 1948). The liquid flow behaviour and distribution of liquid recovered is compared against experimental data.

4.1 Liquid Holdup

Slight liquid holdup hysteresis was observed in the experiments at the lower flow rates. Ilankoon & Neethling (2012) reported that columns that are started flooded will have a higher steady state holdup for the same liquid addition rate compared to those started dry. They demonstrated that the dominant cause of this hysteresis is a change in the number of liquid rivulets flowing through the ore rather than a change in their shape and structure. Hysteresis can be incorporated into the water retention curves by considering two functions, drying and wetting. This requires some scaling from the main wetting curve or additional parameters to describe the hysteresis in the wetting function (Simunek et al, 1999). For the purposes of the modeling work reported here, a single value function between head and water content, i.e. the wetting and drying curves are assumed the same.

4.1.1. Model Calibration

The van Genuchten parameters were obtained by calibrating the simulated liquid holdup and residual moisture to the experimental values. Figures 2 and 3 show both the predicted and measured steady state and residual liquid holdups for the narrowly sized and realistic particle size distributions respectively. The model predicted values could be improved by modifying the residual saturation in time to account for the hysteresis (Mostaghimi et al., 2014a).

However, for general prediction purposes, it is felt that a single set of parameters should be employed for all flow rates.

The narrowly sized particles (20-26.5 mm) had a porosity of 2.16% and when packed resulted in a bulk voidage of 36.3% giving a saturated moisture fraction of 0.363. The density and viscosity of the liquid were 1010 kg/m^3 and 8.9 x 10^{-4} Pa.s. The permeability of the ore was 4.29 x 10^{-9} m^2 giving a calculated saturated conductivity of 4.77 x 10^{-2} ms^{-1}. The water retention curve fitted parameters were n = 4, α = 40 m^{-1} and L = -0.63. As can be seen in Figure 2 the model slightly under predicts the liquid holdup at the lower flow rates and slightly over predicts the liquid holdup at the high flow rate, but overall the model gives a reasonable approximation of the variation in water retention over the range of flow rates investigated.

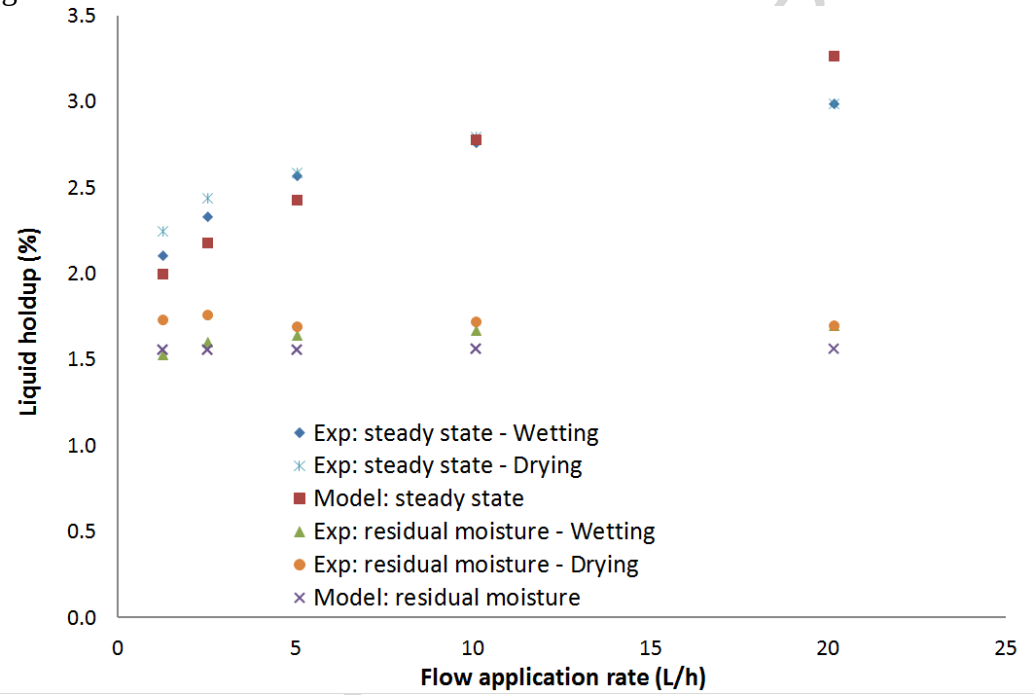

Figure 2: Liquid holdup on narrow sized particle distribution.

The realistic particle size distribution (2-26.5 mm) had a porosity of 4.19% and when packed resulted in a bulk voidage of 28.96% giving a saturated moisture fraction of 0.2896. The density and viscosity of the liquid were 1010 kg/m^3 and 8.9 x 10^{-4} Pa.s. The permeability of the ore was 2.33 x 10^{-9} m^2 giving a calculated saturated conductivity of 2.59 x 10^{-2} ms^{-1}. The water retention curve fitted parameters were n = 3.6, α = 40 m^{-1} and L = -0.5. As can be seen in Figure 3, there is less hysteresis seen in the realistic sized particle distribution and the model predicted holdup is in reasonable agreement with measured values.

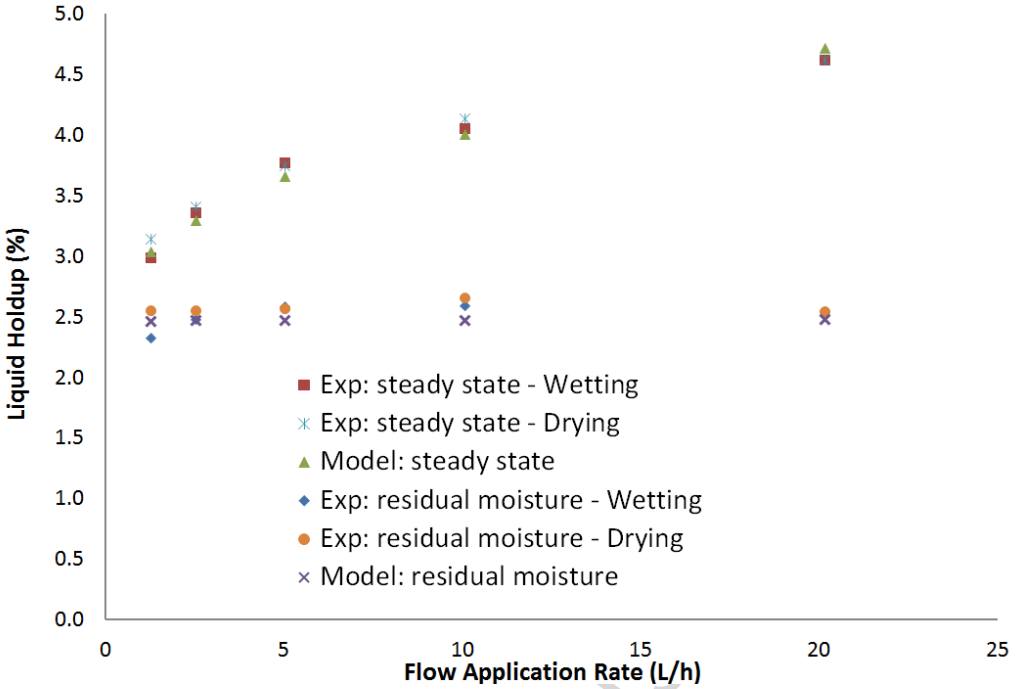

Figure 3: Liquid holdup on realistic sized particle distribution

4.2 Single drip emitter on packed bed

The different simulation setups in this work are illustrated in Figure 4. The geometry of the packed bed was represented by a two-dimensional hexahedral mesh, as shown in Figure 4a. A volume source of 4.2 L/h was introduced into the center element located on the top surface of the mesh. The base of the mesh was split into 25 evenly spaced outlets assuming free drainage conditions. The material properties for each particle size distribution were set to the experimental derived values and the van Genuchten parameters fitted in the one dimensional validation. Figure 4a assumes uniform material properties and voidage giving a homogeneous symmetric system. However, Figure 4b assumes uniform voidage but with volume sink terms applied randomly near the top of the packed bed which allows solution to travel straight to an outlet without interacting with the ore. Figure 4c assumes the same bulk voidage but with local variations allowing a more realistic representation of the packed bed. The local voidage variations were applied to the mesh elements using a uniform distribution.

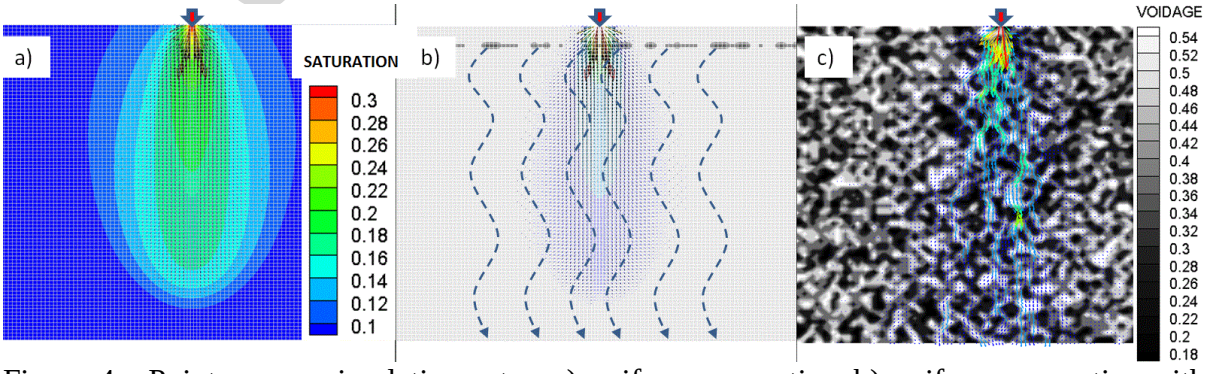

Figure 4: Point source simulation setup a) uniform properties, b) uniform properties with channel pathways, c) Bulk properties unchanged but with local variations in voidage

4.2.1 Narrow-size ore particles

The steady state percent of liquid flow out of the bed at each of the 25 outlet collection points for uniform properties are shown in Figure 5. A near steady state recovery is obtained in the experiments with slight recovery fluctuations occurring and a significant shift in the recovery distribution after 120 hours, observed in Figure 5. However, the experimental results show the liquid behaviour with the bulk volume of fluid being recovered at a couple of collection points with half the fluid being recovered at a single central collection point. The simulation assuming uniform properties predicts recovery at the outlet to be more evenly spread over a parabolic distribution, which agrees with random walk hypothesis. Mathematically Gaussian type probability distribution results at the exit for liquid fed from a point source through the packing media (Scott, 1935; Tour and Lerman, 1939). Furthermore, Dixon (2003) presented narrow Gaussian type liquid spread results around the axis of the dripper by solving the Richards' equation at steady state in 2-D axisymmetric coordinates. Including channelling pathways in the simulation captures the peak in fluid recovery at the centre outlet but predicts asymmetric recovery at the other outlets. Incorporating local voidage variations in the material properties gave a more random distribution at the outlets whilst still capturing the bulk liquid collection point at the centre.

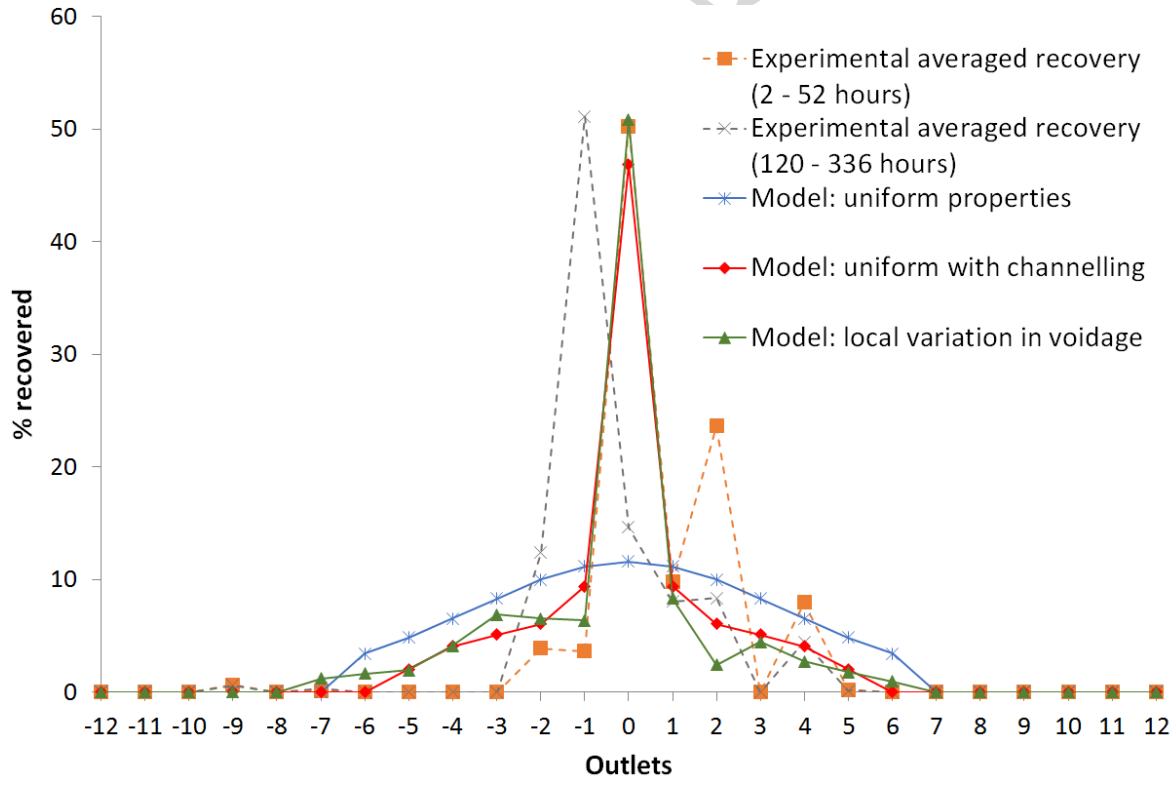

Figure 5: Narrowly-sized particle distribution: Percent of liquid recovered at each outlet

A steady state was never quite reached in the experiments with initial preferential flow paths (gravity dominated flow) forming rapidly whilst the liquid horizontal spread (capillary transport) took many days to reach a near steady state (e.g., 14 days). In the simulations, a steady state was reached in approximately one hour. This is possibly due to the simulations assuming static idealized contact between particles in the packing. Contour plots of the liquid flux and percent of liquid in the ore are shown in Figure 6 for each case simulated. As seen in Figures 6a and 6d, which assume uniform properties, this produces an asymmetric fluid distribution with strong capillary forces acting to spread the solution over a larger area.

Including channelling flow pathways in the simulation provides stronger gravity dominated flow with a strong liquid flux into the channels, Figure 6b. However, liquid not entering the channel pathways is transported through the ore in a similar manner to that seen in the simulation without channelled flow. As can be seen in Figures 6d and 6e, the percent liquid at a steady state is very similar. The simulation with local variations in voidage provides a random pattern to the liquid flux and percent liquid in the ore, Figures 6c and 6f. The liquid is transported predominately by gravity with many interconnected preferential flow paths of varying sizes.

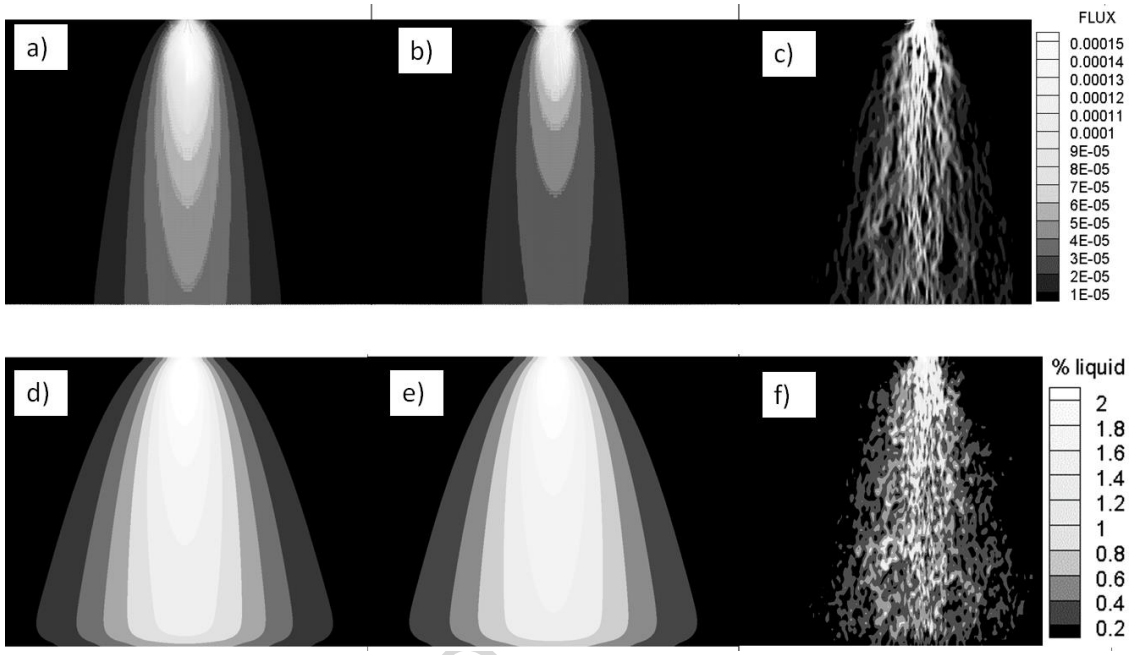

Figure 6: Narrow-sized particle distribution: Contour plots of liquid flux and liquid content, uniform properties a) and d), uniform with channelling b) and e), local variation in voidage c) and f).

The wetted areas of the bed at steady state for the simulations and near steady state for the experiment are shown in Figure 7. For the simulated results, the wetted area was assumed to be the area with moisture levels above the particle micro porosity. Experimentally, the wetted area is seen initially as a narrow region from top to bottom beneath the drip emitter (see Figures 4 and 5 in Ilankoon and Neethling, 2016). Capillary forces spread the liquid horizontally over a 14 day period to cover 61% of the bed. In the simulation of the uniformly packed bed, the particle contact is idealized and the ratio of capillary forces to gravity forces is much stronger, with the inclusion of channelling effects achieving 87% wetting and without channelling 89% wetting. Allowing for local variations in the voidage gave a wetted area much closer to that observed experimentally (61.1% vs 55%).

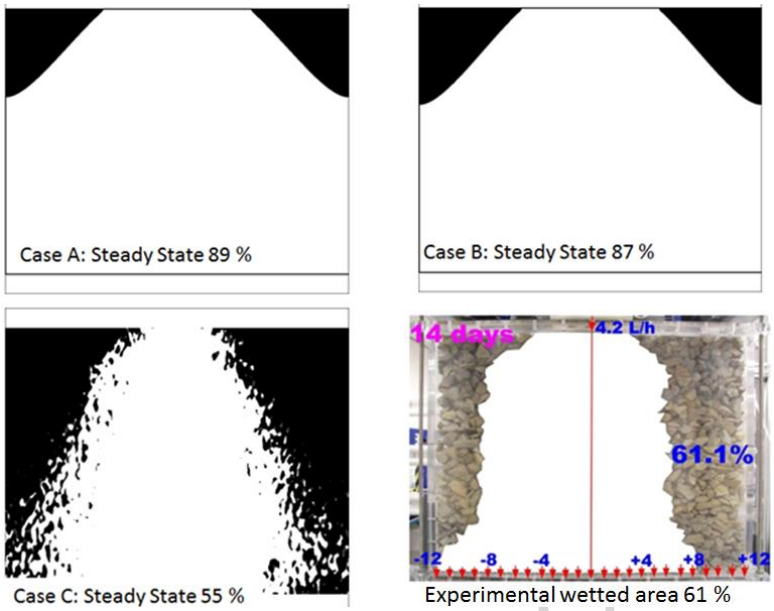

Figure 7: Narrow-sized particle distribution: Wetted area of bed at steady state, uniform properties (Case A), uniform with channelling (Case B), local variation in voidage (Case C), experimental wetted area profile.

4.2.2 Realistic-size ore particles

For the ore with a realistic particle distribution, the distribution of solution recovery at the outlets for the simulations and experiment is shown in Figure 8. The simulated recovery of solution out of the packed bed is spread through a larger number of outlets than in the narrowly sized ore. This is not seen experimentally (3 channels) and also in the experiment the solution exited the ore at a discrete number of non-neighbouring outlets. The simulations predict a continuous spread of solution at the outlets, with uniform properties giving a wider parabolic distribution (agrees with random walk based probability distribution). Including channelling effects gave a central outlet spike in recovery and local voidage variations gave off-centre fluctuations with a peak at the centre outlet. The simulated distribution is probably influenced by the length scale and amplitude of the variation in porosity and a better match might be achieved by calibration of these parameters.

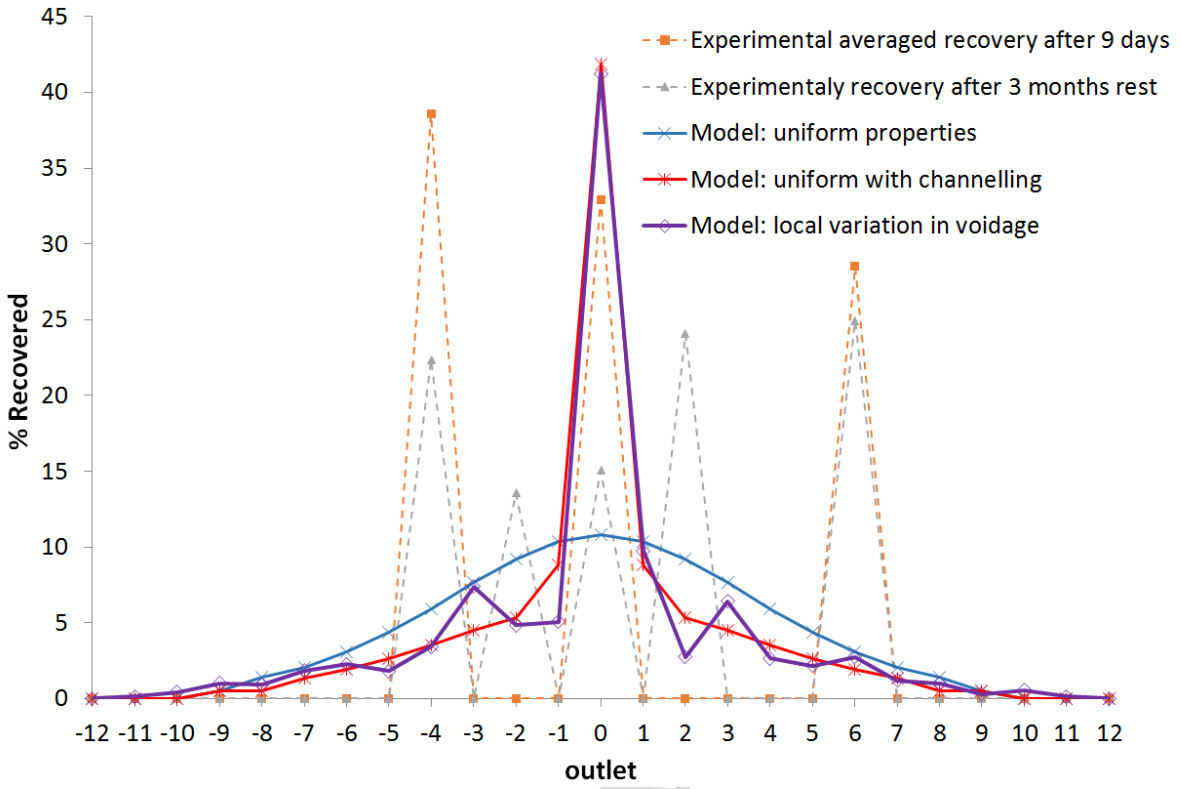

Figure 8: Realistic-sized distribution: Percent of liquid recovered at each outlet

As with the narrowly sized particle distribution, the experiment never quite reached steady state recovery and an occasional shift in the recovery distribution occurred. The experimental recoveries for the initial test and for the test repeated again after the ore had been drained down and rested for 3 months are shown in Figure 8 along with the simulated results. As can be seen in the experimental data, the exact fluid flow path is subject to subtle changes but the general flow channelling behaviour is observed in both tests. Contour plots of the liquid flux and percent liquid in the ore for each case simulated are shown in Figure 9. As seen in the narrow sized distribution, the ore with uniform properties results in asymmetric fluid distribution with strong capillary action. The flux and fluid distribution in the ore with local voidage variations also has a wider solution spread with many preferential flow paths spreading over a much wider area. This is seen experimentally with a wider range of particle sizes allowing more connected inter-particle spreading of liquid, which increases the particles wetted surface area and transport through intra-particle pore space. As can be seen in Figures 9d, 9e and 9f, the liquid spread horizontally through the ore by capillary suction is much greater than that seen in the narrowly sized distribution.

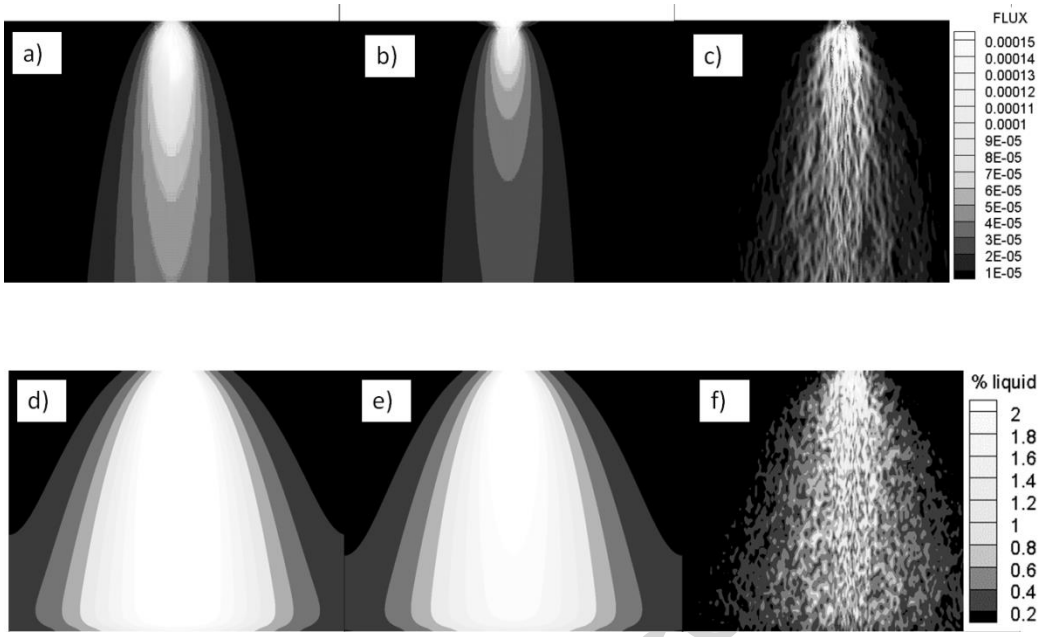

Figure 9: Realistic-sized particle distribution: Contour plots of liquid flux and liquid content, uniform properties a) and d), uniform with channelling b) and e), local variation in voidage c) and f).

The wetted area of the wider particle-sized ore bed is shown in Figure 10 at steady state for the simulations and near-steady state for the experiment. In the experiment, the wetted area rapidly spreads throughout the bed with 63% of the bed wetted after 6 hours (only 21% after the same time in the narrowly sized bed) and 96.5% wetted after 5 days (wetted area of the narrowly sized fraction was 47% after 5 days). The capillary spread of solution is also much stronger in the simulation with the uniformly packed bed achieving 95% wetting and with the inclusion of channelling effects 90% wetting. Allowing for local variations in the voidage gave a reduced wetted area of 84%. However, as the voidage distribution is randomly applied a slightly different configuration would produce a different set of inter-connected pathways, inter-particle contact and intra-particle spreading of solution. The simulation was rerun with a different random voidage configuration which still gave the same bulk voidage, i.e. different specific configuration but same amplitude and length scale. The wetted area for the new voidage configuration was 90%.

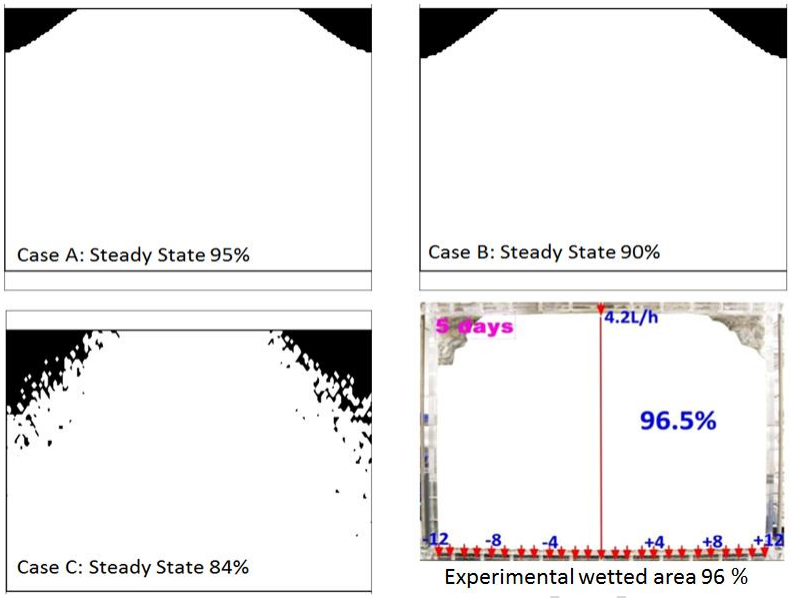

Figure 10: Realistic-sized particle distribution: Wetted area of bed at steady state, uniform properties (Case A), uniform with channelling (Case B), local variation in voidage (Case C), experimental wetted area profile.

4.2.3 Discussion

The techniques employed to account for preferential flow and channelling of solution provided better representation of the solution distribution and recovery at the base of the ore bed than that obtained assuming homogeneous conditions. However, none of the simulations gave an exact match to that seen experimentally. This is not unexpected as small differences occur in the local voidage distribution of each packed bed and slight changes in inter-particle flow are observed over time. Changes in the distribution of liquid recovered at the outlets and the occasional significant shift at the outlet with the highest percentage of liquid recovered is probably due to minor particle shifting or solution fluctuations causing variations in inter-particle flow paths. These slight variations are observed in the experiments (Ilankoon and Neethling, 2016) and can be seen in Figures 5 and 8. They were also observed experimentally by Fagan et al. (2014). However, the critical flow features observed in the experiments are similar, and the simulations accounting for the preferential flow paths have captured these critical features, i.e., initially strong inter-particle flow with little horizontal spread with the bulk liquid exiting at a central outlet followed by slower intra-particle wetting. Accounting for random variations in local voidage distributions, Figures 6c and 9c gave many interconnecting flow paths. This could be further observed in packed bed systems by non-invasive visualization of the flow paths, which is not the objective of the current work. Although this is more in line with the flow path development seen in the experiment, see Figure 10, the inter-particle flow paths observed experimentally had fewer small flow paths and were dominated by a number of stronger flow channels.

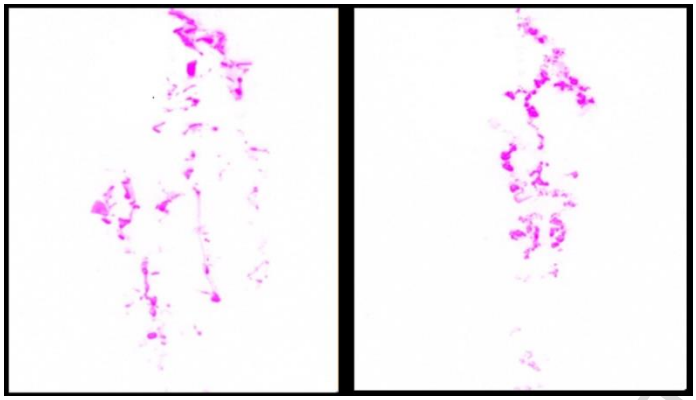

Figure 10: Experimental ultraviolet images of initial flow paths

In the experiments, the inter-particle flow paths form quickly and are reasonably steady within an hour but the intra-particle wetting takes several days to reach a pseudo steady state. The work of Ilankoon and Neethling (2013, 2016) confirm that the difference in time scales of liquid transport through inter-particle voids and intra-particle pore space has a large impact on the flow behaviour in the vicinity of the drip emitters. This difference in time scales is strongly influenced by the particle size distribution with the narrowly-sized fraction having less overall horizontal spread, but more and different flow paths. The intra-particle pore space is a material property which experiments show decreases as the particle size increases. Thus the more realistic size particle distribution, which has a smaller average particle size, has higher intra-particle porosity. Realistically sized distributions with a larger range of particles sizes allow smaller particles to fill the space between larger particles allowing more connected inter-particle spreading of liquid, which increases the particles wetted surface area and transport through the intra-particle pore space. Although numerically a steady state solution was obtained within hours for both size distributions investigated, the difference in the inter-particle spreading of liquid of the different particle sizes was captured. The difference in time scales is probably due to the model failing to capture the differences in inter- and intra-particle permeability. Experimental data shows that the permeability of the saturated particles are a few orders of magnitude smaller than that of the inter-particle spaces and the model does not capture this sharp drop in permeability when the only connections are within the intra-particle spaces. A possible solution would be to employ a dual permeability model with different inter and intra-permeability's.

In general, the techniques investigated to account for channelling in the ore capture the implied fluid behaviour. Assuming uniform properties with random preferential flow channels, where solution travelling in the channels does not interact with the ore, captures the peak in recovery at the central outlet. Only the solution that does not enter the channel pathways is spread through the ore via capillary action. The numerical method that accounts for local variability in the ore void space allows for many inter-connected flow pathways, thus solution can move from inter-particle to intra-particle transport at any point in the ore. For heap leach simulations, both methods initially reduce the solution-ore contact and hence, limit the particle reaction kinetics, thus better representing the physical leaching process in ore stockpiles. However, applying channelling pathways removes a fraction of the solution from being transported by capillary action and reacting with the ore. Applying local spatial variations in voidage allows solution to flow preferentially through conductive regions whilst still interacting with the ore. The effect on the leaching kinetics based on these factors is investigated in a hypothetical leach in the following section.

4.3 SOLUTE TRANSPORT

In order to investigate the effect of employing the techniques detailed in this paper to account for preferential flow and solution channelling on the leaching kinetics in a heap leach simulation, a hypothetical reactant was applied to the realistic sized ore system assuming a simple shrinking core linear reaction. The dispersion coefficient is set to zero, as the aim is to investigate how the solute is transported throughout the ore by the bulk fluid. The rate at which the ore particles react is modelled by equation 7. It is assumed that the dissolution of one mole of mineral requires two moles of reactant. This hypothetical leach employs a simple fast reaction with the species reacting on contact with the reactant. The aim was to investigate how the different channelling assumptions affected the efficiency of the reactant transport and does not represent the complex kinetics of a copper leach.

$$\frac{dr_m}{dt} = -\frac{M_i D_{eff} c_o}{\rho_{ore} x_i} \tag{9}$$

where r_m is the mineral radius, M_i is the molecular weight of the mineral, D_{eff} is the effective particle diffusion coefficient, c_o is reactant concentration, ρ_{ore} is the ore density and x_i is the mass fraction of the mineral.

The simulations assumed one averaged sized particle of radius of 7.78 mm with density of 2700 kg/m^3 and 1 ppm of reactive mineral of molecular weight of 0.1 kg/mol. A particle diffusion coefficient of 1.0 x 10^{-9} m^2/s was assumed. The ore was irrigated with 25 ppm of a reactant of molar mass 26 g/mol at a rate of 4.2 L/h. A single drip emitter was employed with simulation setup as described in section 4.2.

The percent of mineral reacted over time is shown in Figure 11 for the first 8 days. The mineral reacted is reduced in the early stages for both of the simulations accounting for preferential flow and channelling. This is due to solution traveling rapidly through the quickly formed inter-particle flow paths, thus the intra-particle wetting is reduced and hence so is the reactant-particle wetting and mineral dissolution. However, after approximately 4 days the simulation assuming spatially varying voidage increases to the highest percent of mineral reacted and this continues for the rest of the simulation. This is due to the reactant being spread more effectively through the ore due to the large number of inter-connected preferential pathways transporting the solute over a wider region, thus allowing solute to diffuse into the particle micro pores of the non-wetted area. This is probably an over prediction in mineral recovery as the inter-particle flow paths observed experimentally had fewer smaller flow paths and were dominated by a number of strong flow channels which is likely to reduce the reactant-particle interaction. The time scale over which this occurred was also under-predicted in the simulations compared to the experimental values. The simulation with uniform properties and channelling assumes large flow channels where the reactant does not interact with the ore. In both simulations assuming uniform properties, with and without channelling, the reactant spreads slower throughout the ore. After 10 days of leaching the reactant had been transported to 75 %, 71 % and 79 % of the ore bed, increasing to 91 %, 88 % and 97 % after 50 days, for simulations with uniform properties, with channelling and non-uniform properties, respectively.

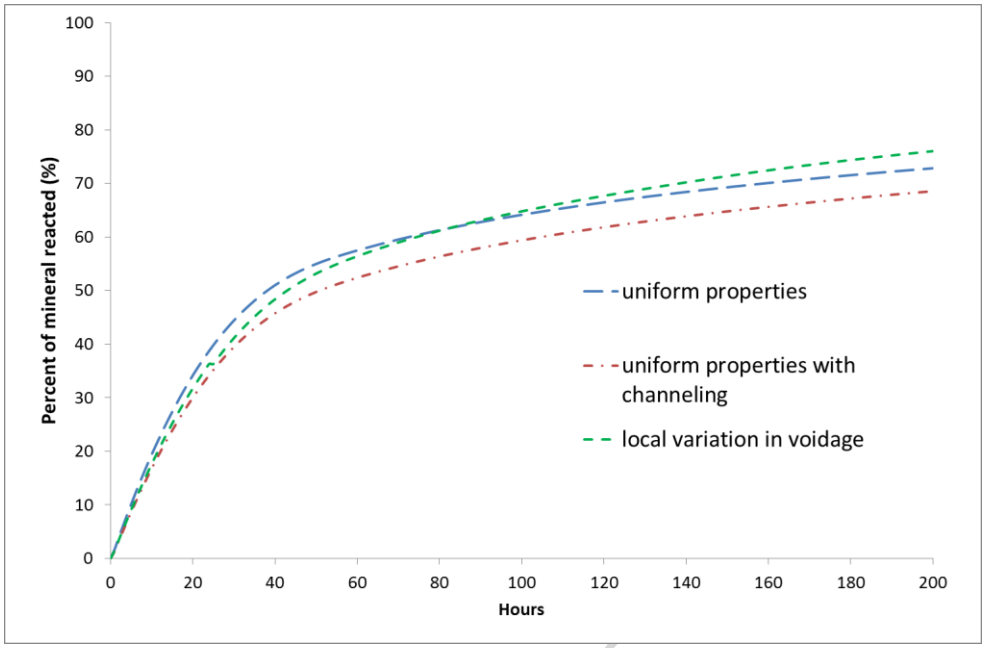

Figure 11: Mineral Recovery variation with time for a hypothetical heap

5. CONCLUSIONS

Experimentally it is shown that gravity driven flow in inter-connected preferential pathways and solution channels establish quickly, whilst horizontal solution transport due to particle-particle contact acts over a much longer time. In industrial heap leaching, the convective transport through inter-connected pathways and channels will dominate the recovery. The slower diffusive transport will spread the reactant to a wider region, but the solution may stagnate locally with the dissolved species not being recovered until later. The spatial delivery of the reactant to different regions of the heap will be highly dependent upon the number of inter-connected preferential flow paths and the scale of the flow channelling. To ensure optimum recovery, the reactant and dissolved species transported by channelling in the ore needs to be eliminated. However in practice, although channelling can be minimized by good packing and heap management, it cannot be completely eliminated and local micro-scale heterogeneities will inevitably occur.

This non-uniform and adverse flow behaviour within the heap reduces the solution-ore contact, and hence, impedes leaching kinetic resulting in lower metal recoveries. Therefore effective modelling of the local flow variations is critical in capturing the leaching kinetics and thus metal recovery. This paper has investigated the implementation of techniques into the CFD model to account for local preferential flow paths in the heap leach system. The results show that the critical behaviour in a pseudo 2-D column, of a narrowly sized ore particles and a more realistic particle size distribution, is comparable to that seen experimentally for the simulations incorporating preferential flow paths. However, the results also highlight the need for good characterization of the ore for recovery predictions. In reality, the network of inter-connecting void space in a heap is inevitably unknown but not accounting for any channelling will clearly lead to an overestimation in the recovered species, especially in the early stages of leaching.

ACKNOWLEDGEMENTS

The experimental tests in this work were performed in the Rio Tinto Centre for Advanced Mineral Recovery at Imperial College London. I. M. S.K. Ilankoon and Stephen Neethling gratefully acknowledge Rio Tinto for their financial support to carry out the experiments.

REFERENCES

Afewu, K.I. (2009). Development and Testing of a 2D Axisymmetric Water Flow and Solute Transport Model for Heap leaching. PhD thesis, University of British Columbia, Canada.

Armstrong, F.E., Evans, G.C., Fletcher, G.E. (1971). Tritiated Water as a Tracer in the Dump Leaching of Copper. US Burequ of Mines, Report of Investiagtions 7510

Bartlett, R.W., 1992, Solution Mining, 2nd Edition, Amsterdam, Netherlands, Gordon & Breach Science Publishers.

Bennett, C.R., McBride, D., Cross, M. & Gebhardt, J.E. (2012). A comprehensive model for copper sulphide heap leaching: basic formulation and validation through column test simulation. *Hydrometallurgy*, 127-128, 150-161.

Bouffard, S.C. & Dixon, D.G. (2001). Investigative Study into the hydrodynamics of heap leaching processes. *Metallurgical and Materials Transactions B, 32,* 763–776.

Bujalski, J.M., Tiller-Jeffery, R.E.,Watling, H.R. and Schwarz, M.P. (2000). CFD Modelling and Comparison with Experimental Residence Time Distributions in Single and Two-Phas Porous Flows. 3rd International Conference on CFD in the Minerals and Process Industries, *CSIRO Minerals*, 463-468.

Bujalski, J.M., Johnson, J., Schwarz, M.P., Watling, H. (2005). Liquid dispersion in model porous media – Comparison of experimental results with computational fluid dynamic modelling. *BioHydrometallurgy05*, Cape Town.

Cariaga, E., Concha, F., & Sepulveda, M. (2005) Flow through porous media with applications to heap leaching of copper ores. *Chemical Engineering Journal*, *111*, 151-165.

Cariaga, E., Martinez, R., & Sepulveda, M. (2015). Estimation of hydraulic parameters under unsaturated flow in heap leaching. *Mathematics and Computers in Simulation, 109*

Cathles, L.M., Murr, L.E. (1980). Evaluation of an experiment involving large column leaching of low grade copper sulphide waste: a critical test of a model of waste leaching process. In: Schlitt, W.J. (Ed.), Leaching and Recovery of Copper from as-Mined Matrials. Societry of Mining Engineers of AIME, Warrendale, PA, 29-48.

Croft, N., Pericleous, K.A. & Cross, M. (1995). PHYSICA: a multiphysics environment for complex flow processes. *In: Taylor, C., Durbetaki, P. (Eds.), Numerical Methods in Laminar and Turbulent Flow'95, 2,* 1269–1280.

Dixon, D.G. (2003). Heap leach modelling – the current state of the art. In: Hydrometallurgy 2003, Proceedings of the 5th International Symposium in honor of Professor Ian M. Ritchie, Volume 1: Leaching and Solution Purification (C.A. Young, A.M. Alfantazi, C.G. Anderson, D.B. Dreisinger, B. Harris and A. James, editors), TMS (The Minerals, Metals & Materials Society), Warrendale, PA, 2003, pp. 289–314.

Dixon, D.G. & Petersen, J. (2003). Comprehensive modelling study of chalcocite column and heap bioleaching. Montreal, Canada, *P.A. Riveros (Ed.*) *et al., Hydrometallurgy of Copper, Proceedings of Copper, 6*, 493–516.

Fagan, M.A., Ngoma, I.E., Chiume, R.A., Minnaar, S., Sederman, A.J., Johns, M.L., Harrison, S.T.L. (2014). MRI and gravimetric studies of hydrology in drip irrigated heaps and its effect on the propagation of bioleaching micro-organisms. *Hydrometallurgy* 150, 210-221.

Garcia, S., Ramon, C., Esplin, A, Gebhardt, J.E, Hernandez, A., McBride, D., and Cross, M. (2010). Gold heap leach simulation and optimization using a multi-physics model, *Minerals & Metallurgical Processing*, 27 (4), 196-204.

Gebhardt, J.E. McBride, D., Bennett, C.R. & Cross, M. (2012). Considering Gangue and Precipitation Reactions within a Copper Heap Leach CFD Model. *International Mineral Processing Congress*, New Delhi, India.

Ghorbani, Y., Franzidis, J-P. and Petersen, J. (2016). Heap Leaching Technology – Current State, Innovations, and Future Directions: A Review. Mineral Processing and Extractive Metallurgy Review: An International Journal, 37(2), 73-119.

Guzman, A., Robertson, S. & Calienes, B. (2013). Constitutive relationships for the representation of a heap leach process, *In: D. van Zyl and J. Caldwell (Eds.), Proceedings of the Heap Leach Solutions Conference*, Vancouver, B.C., 442-458. ISBN: 978-0-9917905-2-4

Howard, E.V. (1968). Chino uses radiation logging for studying dump leaching process. *Minerals Engineering* 70-74

Ilankoon, I.M.S.K., (2012). Hydrodynamics of unsaturated particle beds pertaining to heap leaching. PhD thesis, Imperial College London.

Ilankoon, I.M.S.K., Neethling, S.J. (2012) Hysteresis in unsaturated flow in packed beds and heaps, *Minerals Engineering* 35, 1-8

Ilankoon, I.M.S.K., Neethling, S.J. (2013) The effect of particle porosity on liquid holdup in heap leaching, *Minerals Engineering* 45, 73-80

Ilankoon, I.M.S.K., Neethling, S.J. (2016) Liquid spread mechanisms in packed beds and heaps. The separation of length and time scales due to particle porosity, *Minerals Engineering* 86, 130-139

Kunkel, J. (2008). Heap leach lixiviant flow myth versus reality tailings and mine waste. Design Operation and Disposal, *CRC Press*, 63–72. ISBN 978-0-415-48634-7

Leahy, M. J., Davidson, M. R. & Schwarz M. P. (2005). A model for heap bioleaching of chalcocite with heat balance: Bacterial temperature dependence, *Minerals Engineering*, 18, 1239-1252.

Leahy, M. J., Schwarz M. P. & Davidson, M. R. (2006). An air sparging CFD model of heap bioleaching of chalcocite. *Applied Mathematical Modelling*, *30*, 1428-1444.

Leahy, M. J., Davidson, M. R. & Schwarz M. P. (2007). A model for heap bioleaching of chalcocite with heat balance: mesophiles and moderate thermophiles. *Hydrometallurgy*, *85*, 24-41.

Leahy, M. J., & Schwarz, M. P. (2009). Modelling jarosite precipitation in isothermal chalcopyrite bioleaching columns, *Hydrometallurgy*, 98, 181-191.

Mualem, Y. (1976) A new model predicting the hydraulic conductivity of unsaturated porous media. *Water Resources Res.* 12, 513-522.

McBride, D., Cross, M., Croft, T.N. Bennett, C.R. & Gebhardt, J.E. (2006) Computational modelling of variably saturated flow in porous media with complex three-dimensional geometries, *International Journal for Numerical Methods in Fluids*, *50*, 1085–1117.

McBride, D., Gebhardt, J.E & Cross, M. (2012a). A comprehensive oxide heap-leach model: development and validation. *Hydrometallurgy*, *113-114*, 98-108.

McBride, D., Cross, M., & Gebhardt, J.E., (2012b), 'Heap leach modelling employing CFD technology: A 'process' heap model, *Minerals Engineering*, 33, 72-79.

McBride, D., Croft, T.N., Cross, M., Bennett, C. & Gebhard, J.E. (2014a). Optimization of a CFD - heap leach model and sensitivity analysis of process operation. *Minerals Engineering*, 63, 57-64

McBride, D., Gebhardt, J.E., and Cross, M. (2014b) Utilizing CFD Technology to Capture Multidimensional Thermal-Fluid-Reactive Phenomena in a Heap Leach Operation, CD Proceedings *Int Conf on Heap Leaching*, Lima, Peru.

McBride, D., Gebhardt, J.E., and Cross, M. (2014c) Investigation of Hydrodynamic Flow in Heap Leaching Using a CFD Computational Model. *Proceedings of the 7th International Symposium on Hydrometallurgy*, 1, 455

McBride, D., Gebhardt, J.E., Croft, T.N. and Cross, M. (2016) Modeling the hydrodynamics of heap leaching in sub-zero temperatures, *Minerals Engineering*, *90*, 77-88.

Mostaghimi P, Ilankoon IMSK, Neethling SJ, (2014a), Use of mesh adaptivity in simulation of flow in packed beds - A case study, *Minerals Engineering*, 63, 157-163

Mostaghimi P, Tollit BS, Neethling SJ, Gorman GJ, Pain CCet al., (2014b), A control volume finite element method for adaptive mesh simulation of flow in heap leaching, *Journal of Engineering Mathematics*, 87, 111-121

Munoz, J., Rengifo, P. & Vauclin, M. (1997). Acid leaching of copper in a saturated porous material: Parameter identification and experimental validation of a two-dimensional transport model. *Journal of Contaminant Hydrology*, *27*, 1–24.

Murr, L.E. (1979). Observations of solution transport, permeability and leaching reactions in large, controlled, copper-bearing waste bodies. *Hydrometallurgy* 5, 67-93.

Murr, L.E., Schlitt, W.J., Cathles, L.M. (1981). Experimental observations of solution flow in the leaching of copper-bearing waste. In: SME-AIME Fall Meeting and Exhibit, Denver, Colorado. 1-18.

Nutzmann, G., Maciejewski, S. and Joswig, K. (2002). Estimation of water saturation dependence of dispersion in unsaturated porous media: experiments and modelling analysis. *Advances in Water Resources*, 25 (5), 565-576.

Pantelis, G., Ritchie, A.I.M. & Stepanyants, Y.A. (2002). A conceptual model for the description of oxidation and transport processes in sulphidic waste rock dumps. *Applied Mathematical Modelling*, *26*, 751-770.

Petersen, J. & Dixon, D.G. (2007) Modelling zinc heap bioleaching. *Hydrometallurgy, 85*, 127-143.

Petersen, J. (2015) Heap leaching as a key technology for recovery of values from low-grade ores – A brief overview. *Hydrometallurgy*, doi:10.1016/j.hydromet.2015.09.001

Richards, L.A. (1931). Capillary conduction of liquids through porous mediums. *Physics*, 1 (5) 318-333.

Roman, R.J., (1977). Solution channelling in leach dumps. Transactions of Society of Mining Engineering, AIME 262, 73-74.

Schaap, M.G., Leij, F.J. (2000). Improved prediction of unsaturated hydraulic conductivity with the Mualem-van Genuchten model. *Soil Sci. Soc. Am. J.* 64, 842-851.

Scott, A.H., 1935. Liquid distribution packed towers. Transactions of the American Institute of Chemical Engineers 13, 211-217.

Simunek, J., Kodesova, R., Gribb, M.M. and van Genuchten, M.T. (1999) Estimating hysteresis in the soil water retention function from cone permeameter experiments. *Water Resources Research*, 35 (5), 1329-1345

Simunek J, Jarvis, N.J., van Genuchten, M.Th., and Gardenas, A. (2003) Review and comparison of models for describing non-equilibrium and preferential flow and transport in the vadose zone, *Journal of Hydrology*, 272 (1-4), 14-35.

Taylor D, W. (1948) Fundamental of soil mechanics, John Wiley & Sons, New York.

Thoma M.J., Barrash W., Cardiff M., Bradford J. and Mead J. (2014) Estimating Unsaturated Hydraulic Functions for Coarse Sediment from a Field-Scale Infiltration Experiment. Vadose Zone J. 5, 877-885.

Tour, R.S., Lerman, F., (1939). The unconfined distribution of liquid in tower packing. Transactions of the American Institute of Chemical Engineers 35, 719-742.

Van Genuchten, M. Th. (1980) A closed-form equation for predicting the hydraulic conductivity of unsaturated soils, *Soil Science Society of America Journal, 44*, 892-898.

Wu, A.,Yin, S., Yang, B., Wang, J., Qiu, G. (2007). Study on the preferential flow in dump leaching of low grade ores. *Hydrometallurgy, 87*, 124–132.

Wu, A. X., Yin, S., Qin, W., Liu, J., & Qiu, G. (2009) The effect of preferential flow on extraction and surface morphology of copper sulphides during heap leaching, *Hydrometallurgy, 95*, 76–81.

Wu, A., Liu, J.,Yin, S. & Wang, H. (2010). Analysis of coupled flow-reaction with heat transfer in heap bioleaching processes. *Applied mathematics and Mechanics, English Edition. 3(12)*, 1473–1480.

Yusuf, R., (1984). Liquid flow characteristics in heap and dump leaching. M.Sc. Thesis. University of New South Wales, Australia.

Zhan, G., Haggarty, S. & Ludwick, W. (2012). Hydrological Evaluation of Gold Leach Pad Rinsing. *Mine Water and the Environment, 31*, 307-311.

HIGHLIGHTS

- Experimental data shows liquid spread and flow channel development in packed beds
- Techniques are incorporated into CFD numerical model to capture flow channelling
- Results show capture of channel flow paths comparable to that seen experimentally
- Simulation of a drip leach shows channelling assumptions effect on solute transport